Tailoring coupling of light to local plasmons by using Ag nanorods/structured dielectric/mirror sandwiches

Motofumi Suzuki[a], Yoshikatsu Imai[a], Hiroki Tokunaga[a], Kaoru Nakajima[a], Kenji Kimura[a], Takao Fukuoka[b], and Yasushige Mori[c]

[a]Department of Micro Engineering, Kyoto University, Kyoto 606-8501, Japan;
m-snki@me.kyoto-u.ac.jp
[b]JST Kyoto Pref. CREATE, Seika, Kyoto 619-0237, Japan;
[c]Department of Chemical Engineering and Materials Science, Doshisha University,
Kyotanabe, Kyoto 610-0394, Japan

Abstract. The optical properties of the sandwich of Ag nanorod array (NRA)/structured dielectric layer/Ag mirror have been investigated theoretically and experimentally, where the structured dielectric layer has stacked sublayers of an anisotropic nanocolumnar layer and a uniform layer. The functions of the nanocolumnar and the uniform sublayers are to control shape of the Ag nanorods and to tune optical path length inside the sandwich, respectively. Calculations based on a simple model by treating the NRAs as uniform effective media indicate that the antireflection condition is realized by changing the thickness of the dielectric layer and that the Ag nanorods absorb most of the incident light. The designed structures have been successfully fabricated by taking advantages of the dynamic oblique-angle deposition technique. Under the experimental antireflection condition, Raman scattering measured on the Ag NRA in the near infrared region exhibits significant enhancement. This indicates that the local electric field close to the Ag nanorods can be controlled by the interference of light in the nanostructured sandwiches.

Keywords: surface-enhanced Raman spectroscopy, oblique-angle deposition, nanorod, columnar thin films, local plasmon

1 INTRODUCTION

Local plasmons in noble-metal nanoparticles are attracting much attention because of their usefulness for biochemical sensing [1], microfluidic mixing [2], and optoacoustic applications [3] etc. Many of these studies aim to use the local plasmons with biomaterials. In order to avoid the fluorescence of biomaterials and the significant optical absorption by water, the nanoparticles employed are often required to resonate in the near-infrared (NIR) region [4].

Recently, we have succeeded in aligning elongated metal nanoparticles, called nanorods, by a physical self-assembling technique, namely, dynamic oblique-angle deposition (DOD) [5]. The nanorod arrays (NRAs) prepared by DOD exhibit the plasmon resonance in the NIR region and excellent surface-enhanced Raman scattering (SERS) properties [6]. However, since the incident light is reflected by or transmitted through these NRAs even at the energies of the local plasmon resonance, the incident light energy is not used efficiently to enhance the local electric field.

On the other hand, for the visible region, it has been reported that Ag island films can be tailored to absorb almost all incident photon energy at a specific wavelength by using the interference structures of Ag islands/dielectric layer/Ag mirror sandwiches [7]. The evidences of the local-field enhancement have also been reported [8–10]. It is known that in order to achieve strong interference, high-density nanoparticle arrays are required [7]. Since one could
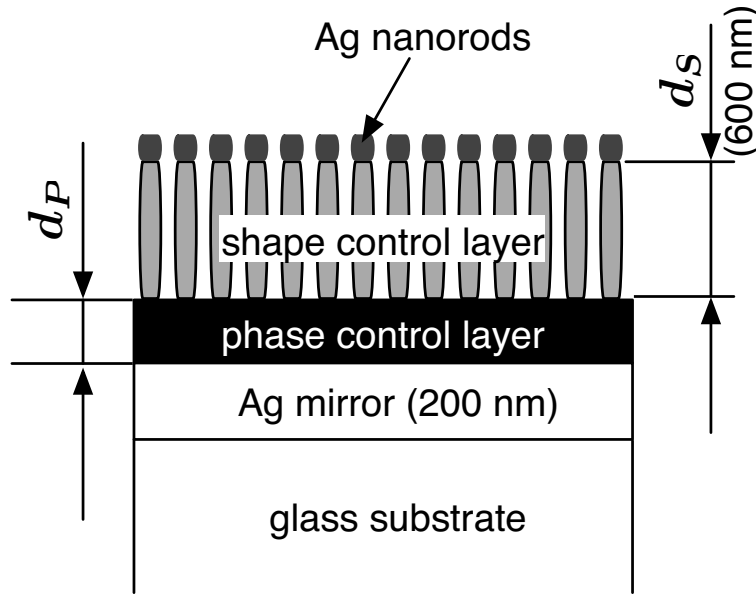
Send correspondence to M. Suzuki

Fig. 1. Schematic drawing of model structure.

not produce such high-density nanoparticle arrays appropriate for NIR applications, no attempt has been made to extend this technique, namely, the use of sandwiches to NIR region.

In this paper, we theoretically discuss the optical properties of Ag NRA/structured dielectric layer/Ag mirror sandwiches. In addition, we report the experimental results of the measurements of the optical reflectance and the SERS properties for the nanostructured sandwich films prepared by DOD.

2 DESIGN OF NANOSTRUCTURES

In this section, we theoretically propose multilayered structures to enhance the coupling of light to the local plasmons in nanorods by using a very simple model. Figure 1 schematically shows the model multilayered structure. For precise tuning of the coupling of light to the local plasmons, it is important to control the distance between the nanorods and the mirror surface [7]. On the other hand, the plasmonic properties of the NRAs prepared by DOD depend strongly on the thickness of the underlying SiO_2 template layer, since the shape of the nanorods reflect the anisotropic surface morphology of the template, which develops depending on the thickness of the template [11]. It is difficult to change only the thickness of the template layer while preserving the optimum shape of the nanorods. Therefore, we consider a multilayered spacer layer comprising two layers that perform the following functions: (1) to control the shape of nanorods and (2) to control the optical path length. In this paper, we name these two layers as the "shape control layer (SCL)," which corresponds to the template layer in our previous paper [11], and the "phase control layer (PCL)," respectively. We calculated the normal-incidence reflectance for the multilayered structures of Ag NRA/SCL/PCL/Ag mirror by using a transfer matrix method developed for birefringent thin films [12].

In the present calculation, the NRA and SCL are treated as anisotropic homogeneous media. Since the SCL has anisotropic nanocolumnar morphology, it is assumed to be a biaxial medium, in which one of the principal axes is perpendicular to the surface and the others are in plane. For the normally incident light, we assumed the in-plane dielectric constants of $\varepsilon_{s'}$ and $\varepsilon_{p'}$ for SCL, where the s' and p' symbols represent the polarizations defined in the next section. The NRA is treated as an effective medium of the mixture of a metal nanospheroid whose major axis is parallel to the s'- polarization, and transparent material. For the simplicity, we assumed that the

metal nanospheroid are embedded in the transparent material with the same dielectric constants with the SCL. Effective dielectric functions for i' ($i' = s'$ or p') polarization are evaluated by the Maxwell-Garnett model as

$$\epsilon_{i'}^{av} = \epsilon_{i'} \frac{\{f + (1-f)g_{i'})\}\varepsilon_m + (1-f)(1-g_{i'})\varepsilon_{i'}}{(1-f)g_{i'}\varepsilon_m + \{1 - (1-f)g_{i'}\}\varepsilon_{i'}}, \tag{1}$$

where ε_m is the dielectric function of the metal; $\varepsilon_{i'} = \varepsilon_{s'}$ or $\varepsilon_{p'}$; f, the volume fraction of the nanorods; and $g_{i'}$, the geometric factor as

$$g_{s'} = \frac{1}{m^2 - 1} \left[\frac{m}{2(m^2-1)^{1/2}} \ln \left\{ \frac{m + (m^2-1)^{1/2}}{m - (m^2-1)^{1/2}} \right\} - 1 \right], \tag{2}$$

and

$$g_{p'} = \frac{1}{2}(1 - g_{s'}). \tag{3}$$

Here m (≥ 1) is the aspect ratio of the nanorods. The dielectric function of the metal is represented by the Drude model $\varepsilon(\omega) = \varepsilon_\infty - \omega_p^2/\{\omega(\omega + i\delta)\}$, where ω_p is the plasma frequency, ε_∞ is the dielectric constant at high frequency, and δ is the reciprocal of the scattering time.

The parameters for the SCL and NRA were chosen so as to reproduce the observed optical properties of the NRA/SCL [13]. In the case of a Ag NRA appropriate for NIR SERS, the amount of Ag in the NRA is 8 nm in weight thickness. From the SEM observations, the volume fraction of Ag is estimated as $f \sim 0.3$, so that the geometrical thickness of the NRA is set at 27 nm. In addition, m is also estimated as 3.5 from the SEM observations. For the metal nanorods, the bulk values of $\omega_p = 9.6$ eV and $\varepsilon_\infty = 5.27$ are adopted [15, 16], while δ was set at 1.5 eV, which is much larger than the bulk value, by taking account of an increase in the scattering probability due to the low crystallinity and surface roughness of the nanorods. A typical SCL consists of SiO_2 and its thickness is $d_S = 600$ nm. From the interference fringe found in the absorbance spectra of the NRA prepared on a glass substrate, the dielectric constants of the SCL were selected as $\sqrt{\varepsilon_{s'}} = n_{s'} = 1.25$ and $\sqrt{\varepsilon_{p'}} = n_{p'} = 1.20$. These values are much smaller than that of bulk SiO_2, since the packing density of an SCL is small [14]. The calculated absorbance spectra are shown in Fig. 2. The spectra consist of a broad absorption band due to the plasmon resonance; small periodic undulation caused by interference is superimposed on this band. These features agree well with those of a Ag NRA prepared on the glass substrate [13].

The Ag mirror (200-nm thick) and the PCL are assumed to be isotropic media with bulk dielectric properties. The dielectric function of the Ag mirror is also represented by the Drude model, although the value of δ for the Ag mirror is 0.0544 eV. On the other hand, the PCL is assumed to be transparent material with a refractive index of $n_P = 1.5$, which corresponds to that of SiO_2. The reflectance spectra of the multilayered structures of Ag NRA/SCL/PCL/Ag mirror were calculated as a function of the thickness of the PCL, d_P.

Figure 3 shows the results of the calculations for (a) selected polarization and d_P and the spectra as a function of d_P for (b) s'- and (c) p'-polarizations. The reflectance changes periodically as a function of the photon energy at a certain value of d_P as shown in Fig. 3(a). As a function of d_P, the reflectance-peak positions changes along white lines and form striped patterns as shown in Figs. (b) and (c). The white lines indicate the following relation,

$$d_P = \frac{1}{n_P}\left(N\frac{\lambda}{2} - n_{i'}d_S \right), \tag{4}$$

where λ is the wavelength in vacuum and N is an integer. For both the s'- and p'-polarizations, the reflectance near these lines is large, while that between the lines is small. This result clearly
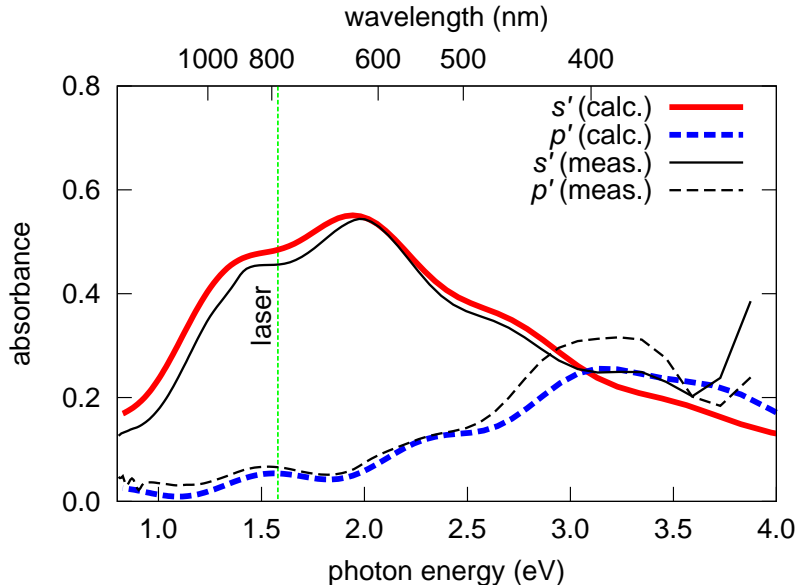
Fig. 2. Calculated and measured [13] absorbance spectra of Ag NRA/SCL prepared on a glass substrate for s'- and p'-polarized light.

indicates that the reflectance of the nanostructures under consideration changes significantly due to the interference. In addition, for s'-polarized light, the reflectance becomes extremely small for certain combinations of d_P and the photon energy in the NIR and visible range. On the other hand, the reflectance of p'-polarized light is considerably large in the NIR region. It is apparent that this strong polarization dependence of the reflectance is closely related to the absorption by the NRA.

In order to clarify the detailed mechanisms of the above mentioned large change in the reflectance, we calculated the field distribution for the specific combinations of the photon energy of 1.24 eV and d_P. Fig. 4 shows the electric field strength for s'-polarized light for (a) $d_P = 215$ nm and (b) $d_P = 135$ nm. The photon energy for both the cases is 1.24 eV. When $d_P = 215$ nm, there exists a standing wave in the spacer layer of SCL/PCL, while the electric field strength is almost constant in air. This suggests that once the light is incident on this multilayered structure, it is absorbed by the NRA during the multiple reflections inside the Ag NRA–SCL/PCL spacer–Ag mirror cavity. As a result, the reflectance becomes extremely small, less than 10^{-3}. On the other hand, in the case of $d_P = 135$ nm, there exists a standing wave in the entire space in front of the Ag mirror. The NRA is located exactly at one of the nodes of this standing wave. As a result, the NRA does not absorb the light significantly and becomes almost transparent. The reflectance under these conditions is 97% or larger.

It has been already reported that the reflectance of a Ag islands/SiO$_2$/Ag mirror sandwich is significantly modified in the visible region due to the same mechanism as we described above [7]. By replacing the isotropic Ag islands with the anisotropic NRA, the coupling of the light to the local plasmons in the NIR region can be modified. In addition to the red-sifted plasmon resonance, strong polarization dependence of the plasmon resonance is also realized by aligning the nanorods in-line. In addition, the resonance width becomes narrow by using a rather thick spacer layer. Under the condition where the most of the light is absorbed by the NRA, strong dipoles are induced in the nanorods; therefore, the local field is expected to be enhanced significantly. This will be useful for biochemical sensing such as SERS.
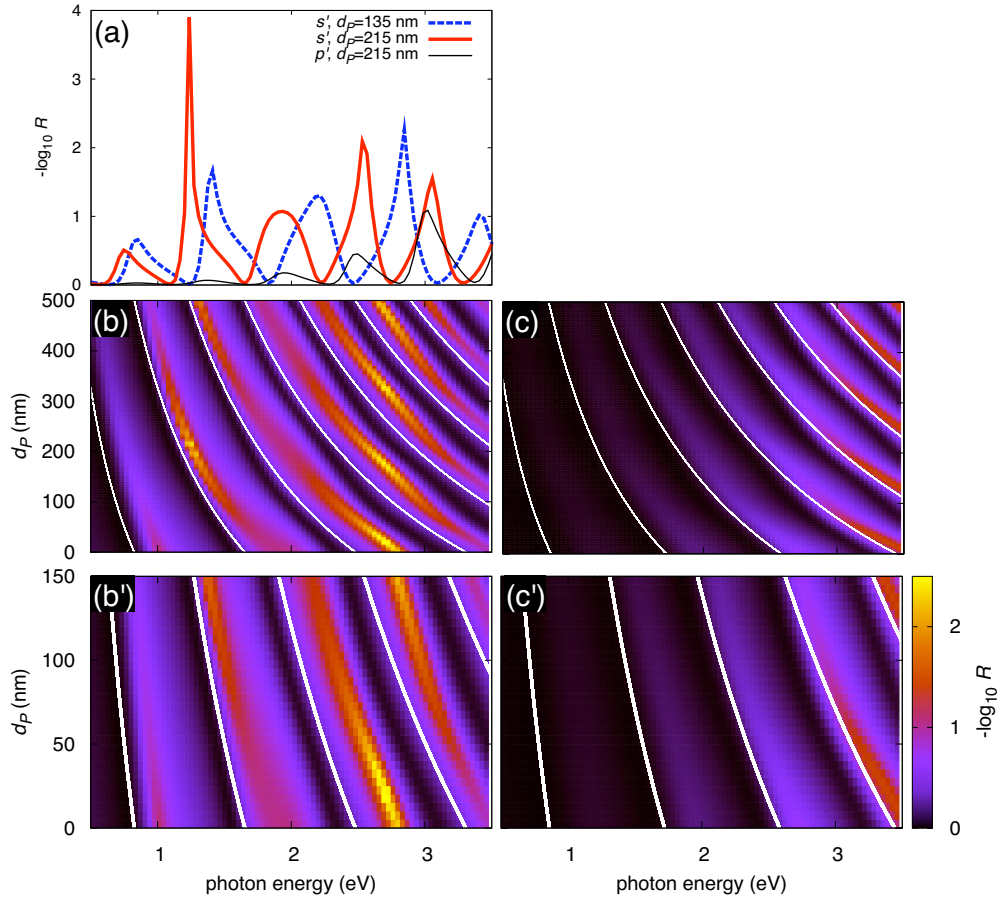
Fig. 3. Calculated reflectance spectra for (a) selected polarization and d_P and those as a function of d_P for (b) s'- and (c) p'-polarizations. (b') and (c') are the magnified version of (b) and (c), respectively, for comparison with the measured spectra. White lines in (b), (c), (b') and (c') indicate $d_P = (N\lambda/2 - n_{i'}d_S)/n_P$, where $N = 1, 2, 3...$; $i' = s'$ or p'; and λ is the wavelength in vacuum.

3 EXPERIMENTS

The multilayered structures designed in the previous section were prepared experimentally. On a glass substrate, a smooth Ag layer of 200-nm thickness was deposited. On this Ag mirror surface, a PCL of SiO_2 of 0–150-nm thickness was deposited with the vapor incident normally to the surface. A series of different SiO_2 thicknesses were realized on a single substrate by moving a shutter incrementally across the sample during the SiO_2 deposition. On the PCL, a Ag NRA was prepared by the same procedure reported in our previous papers [6,13]. In order to control the shape of the Ag nanorods, a SCL of SiO_2 with an anisotropic surface morphology, which was called as the "template layer" in our previous paper, was prepared by the serial bideposition (SBD) technique [17]. A tablet of SiO_2 (purity 99.9%) was evaporated from an electron-beam (EB) source placed at a distance of 480 mm from the substrate under a pressure of 7×10^{-3} Pa. During the SBD, the deposition angle α_{SiO_2} measured from the surface normal was fixed at an angle of $79°$, while the azimuthal angle ϕ was changed rapidly by $180°$ with each deposition of an approximately 20-nm-thick layer. After 15 cycles of SBD, a SiO_2 layer with an approximate thickness of 600 nm was obtained. Onto this fabricated template layer,
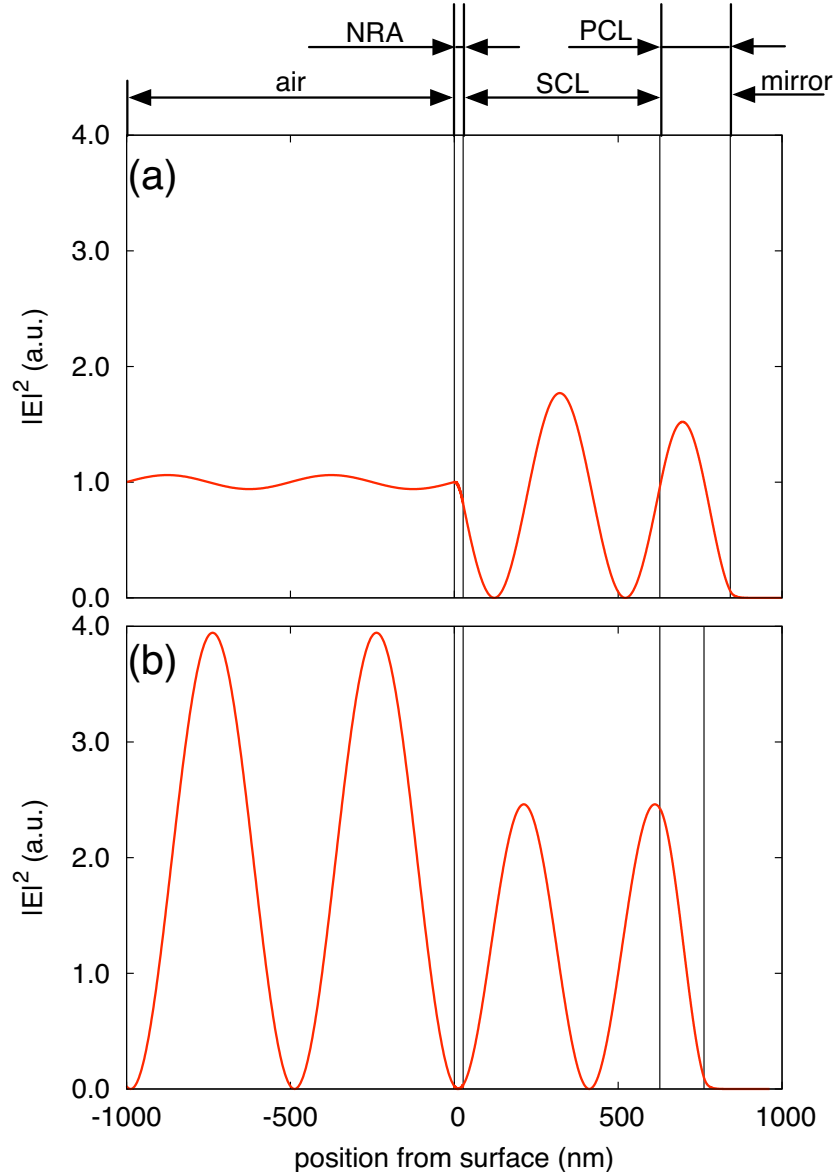
Fig. 4. The electric field strength for s'-polarized light as a function of the position from the surface of the multilayered structure. (a) $d_P = 215$ nm and (b) $d_P = 135$ nm. For both cases, the photon energy is 1.24 eV. The vertical lines indicate the positions of the interfaces.

Ag was deposited obliquely. The pressure during the Ag deposition was 3×10^{-4} Pa, and the vapor flux of Ag was 0.1–0.2 nm/s. The deposition angle of Ag, α_{Ag}, was set at $73°$, while the azimuth remained unchanged during the Ag deposition. The amount of deposited Ag was 8 nm in average thickness, which was so minute that the Ag layers remained discontinuous on the template.

The optical reflectance of the samples was measured using a single-beam spectrophotometer as a function of the thickness of the SiO$_2$ PCL, d_P, in the wavelength range 300 nm $< \lambda < 1700$ nm at an angle of incidence of about $3°$. On the basis of the study carried out by Hodgkinson and Wu [12, 18], the polarization of the incident light was defined as either p' or s' in which the electric field vibrates parallel or perpendicular to the *deposition plane* of SiO$_2$ and Ag,
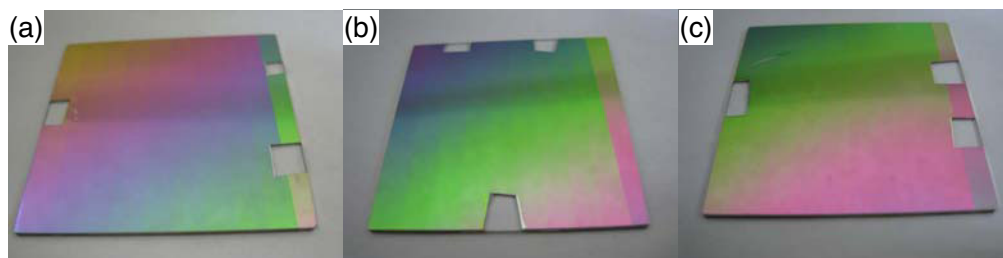
Fig. 5. Visual appearance of the samples (a) 0 nm $\leq d_P \leq$ 50 nm, (b) 50 nm $\leq d_P \leq$ 100 nm, and (c) 100 nm $\leq d_P \leq$ 150 nm. The value of d_P increases from left to right.

respectively. Since the nanorods were elongated perpendicular to the deposition plane p'- and s'-polarizations corresponded to the polarizations perpendicular and parallel to the nanorods, respectively. In order to avoid confusion with the ordinary definition of the polarization, which is associated with the plane of incidence of light, we have used the prime symbol to indicate the polarization associated with the deposition plane in this paper.

Raman spectroscopy was carried out using a NIR confocal Raman microscope (The LabRam 1B, HORIBA Jobin Yvon) at an excitation wavelength of 785 nm and a power of 1.5 mW. The microscope had a $60\times$ objective (NA = 0.7) and a confocal pinhole with a diameter of 1.1 mm. In order to perform *in situ* SERS measurements on the Ag NRAs immersed in a 4,4$'$-bipyridine (BiPy) water solution, we created a small cell (6-mm diameter with a spacer of silicone rubber of 0.5-mm thickness) on the sample. After the cell was filled with the BiPy solution, it was sealed with a cover glass. The excitation laser was polarized by a commercial polaroid film with an extinction ratio of 170 at $\lambda = 785$ nm.

4 RESULTS AND DISCUSSION

Figure 5 shows the visual appearance of the samples with the phase control layers of different thicknesses. For these samples, the value of d_P increases from left to right. The samples are vividly colored depending on d_P. Figure 6 shows the typical SEM images of the multilayered structures of Ag NRA/SCL/PCL/Ag mirror. The SEM image of the cross section fractured parallel to the deposition plane of the SiO_2 and Ag fluxes exhibits narrow and long columnar structures with small zigzag in the SCL and the uniform layers of the PCL and Ag mirror [figure 6(a)]. On the contrary, the cross section fractured perpendicular to the deposition plane of the SiO_2 flux, which is not shown here, contains thick bundles of columnar structures [11]. As a result, the surface exhibits anisotropic corrugation [figure 6 (b)]. The anisotropic morphology of the SCL is physically self-assembled without the use of any lithographic techniques. As indicated by the arrow in figure 6 (b), Ag was deposited in the downward direction in this image so that the Ag nanoparticles grow on the top and slightly toward the upper sides of the elongated columns of the template due to the shadowing effect of the surface corrugation. The morphologies of the SCL and NRA are almost the same as those of the samples without PCL and Ag mirror reported in our previous papers [6, 11, 13]. The multilayered structures designed in Sec. 2 are successfully realized. It is quite useful for tuning the plasmonic properties that various combinations of the materials and the morphologies are possible if we use the DOD technique without any pre- and post-processing [19].

Figure 7 shows the polarization dependent reflectance spectra as a function of d_P. Clearly, striped patterns are observed in Figs. 7(b) and (c), in which the reflectance changes periodically as a function of the photon energy at a certain value of d_P as shown in Fig. 7(a). The reflectance in the NIR region for s'-polarized light is much larger than that for p'-polarized light. Among the conditions wherein the reflectance becomes small, we found the antireflection conditions for s'-polarized light. On the other hand, the maximum values of the reflectance are very close
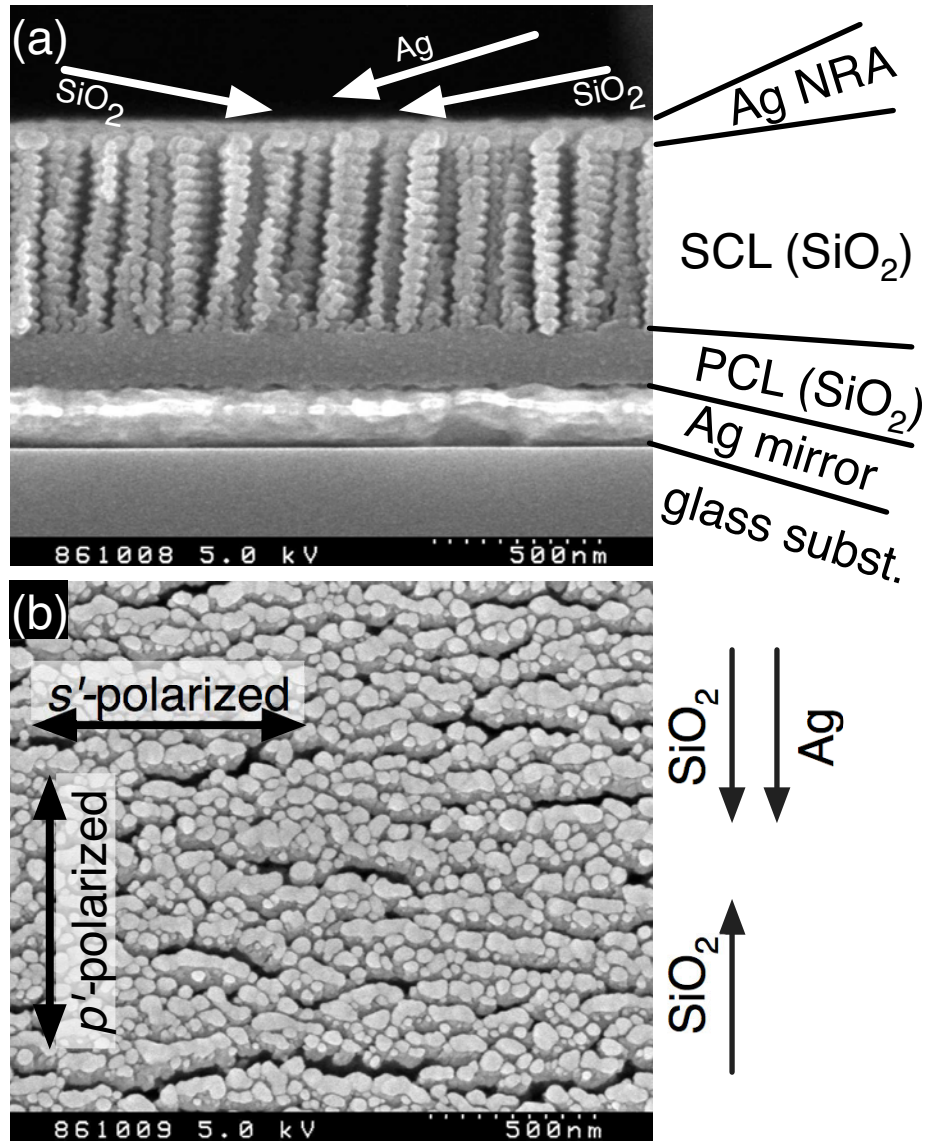
Fig. 6. SEM images of (a) cross section and (b) surface of Ag NRA/SCL/PCL/Ag mirror structure. Arrows indicate the incident directions of SiO_2 and Ag for NRA. The polarization directions are also indicated on (b).

to 100%. For example, the reflectance on $d_P = 125$ nm for s'-polarized light becomes smaller than 1% at a photon energy of around 1.5 eV, while that on $d_P = 0$ nm at the similar photon energy becomes approximately 100% as shown in Fig. 7(a). Comparing the measured spectra [Figs. 7(b) and (c)] with the calculated ones [Figs. 3(b') and (c')], the features of the measured reflectance are quite similar to those calculated ones as we described in Sec. 2. Therefore, the coupling of the light to the local plasmons in Ag nanorods is successfully modified by interference, although the precise peak positions are slightly different with each other, perhaps, due that the model is very much simplified.

In general, a dipole induced in metal nanoparticles by the incident light radiates the scattering light or absorbs the incident light. Thus, the intensity of the scattered light and absorption are good indexes of the strength of the induced dipole. However, in the present case, the intensity
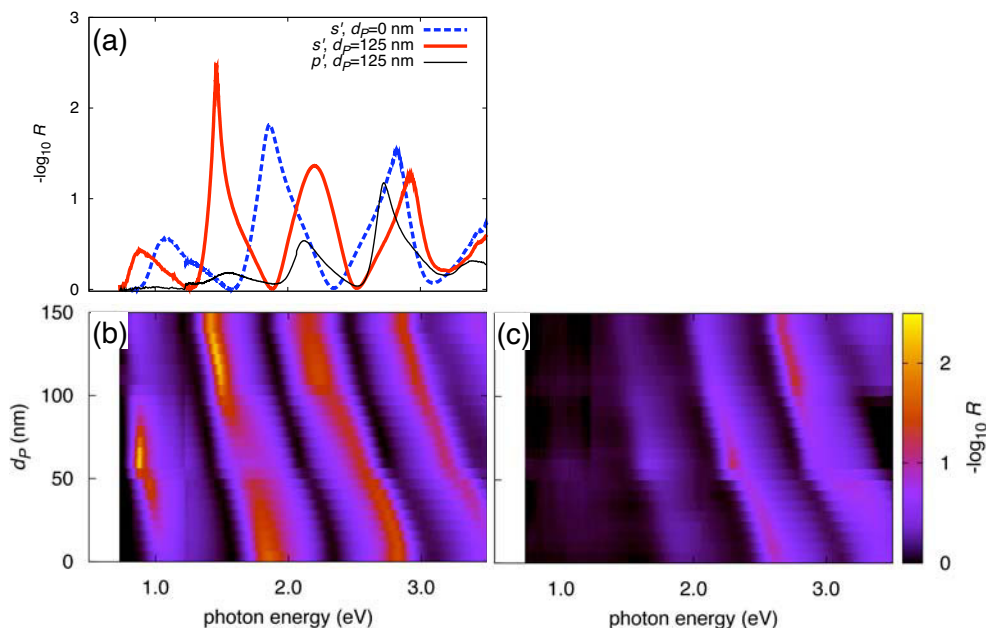
Fig. 7. Measured reflectance spectra for (a) selected polarization and d_P and those as a function of d_P for (b) s'- and (c) p'-polarizations.

of the scattered light is strongly influenced by the interference; therefore, only the absorption corresponds to the intensity of the induced dipole. Under the antireflection conditions, the incident light is confined within the multilayered structures, and most of the light is absorbed by the Ag nanorods. Therefore, the local electric field close to the Ag nanorods is expected to be enhanced significantly.

In fact, the Raman scattering of the BiPy solution measured on the present multilayered structures are significantly enhanced. Figure 8 (a) shows the SERS spectra measured on the samples with different d_P and that measured on the NRA prepared on the glass substrate. The clear peaks observed are the characteristics of the SERS of BiPy on noble-metal particles [20]. The SERS intensity measured on the sample of $d_P = 106$ nm is 26 times stronger than that on the sample of $d_P = 19$ nm. As we have reported in our previous paper, Raman scattering for s'-polarized light is enhanced significantly. Even on the NRA prepared on the glass substrate, an enhancement factor larger than 10^7 is available [6]. Remarkably, the SERS intensity measured on the sample of $d_P = 106$ nm is 65 times stronger than that measured on the sample prepared on the glass substrate.

Figure 8 (b) shows the dependence of the SERS spectra on d_P. The SERS intensity systematically depends on d_P and becomes large when 60 nm $\leq d_P \leq 125$ nm. Comparing with the reflectance spectra shown in Fig. 7 (a), it is found that SERS is strong for the samples with low reflectance. Therefore, the local electric field is enhanced by concentrating the light by using the interference phenomenon.

5 CONCLUSION

The optical properties of Ag NRA/SCL/PCL/Ag mirror strictures have been investigated theoretically and experimentally. The calculations based on the simple model, in which the Ag NRAs are treated as an effective medium, indicate that the reflectance in the NIR region can be controlled between 10^{-4} and ~ 1 by changing the thickness of the PCL. At low reflectance conditions, due to the strong interference, the Ag nanorods absorb most of the incident light and are
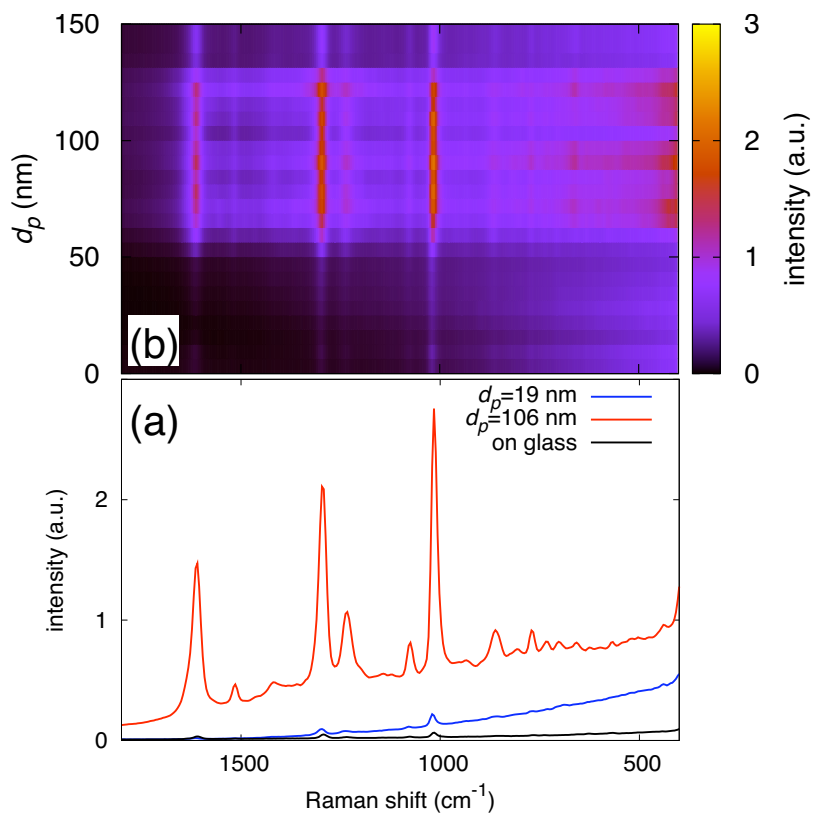
Fig. 8. SERS spectra (a) for the selected samples and for the samples prepared on the glass substrate and (b) as a function of d_P. The incident laser has s'-polarization.

expected to enhance the local electric field in their close vicinity. The designed structures were experimentally realized by the DOD technique. The reflectance spectra measured as a function of the PCL thickness agree well with the calculated ones. The SERS intensity measured on the present samples with low reflectance is 65 times stronger than that on the Ag NRA prepared on the glass substrate. This indicates that the local electric field in the NIR region is controllable by using interference. Therefore, the NRA fabricated on the mirror with appropriate spacer layers is useful not only for improving conventional biochemical sensing but also for the novel applications using spatiotemporal control of the local plasmons.

Acknowledgment

References

[1] D. L. Jeanmaire and R. P. Van Duyne, "Surface Raman spectroelectrochemistry part I. heterocyclic, aromatic, and aliphatic amines adsorbed on the anodized silver electrode," *J. Electroanal. Chem.* **84**, 1–20 (1977) [doi:10.1016/S0022-0728(77)80224-6].

[2] X. Miao, B. K. Wilson, and L. Y. Lin, "Localized surface plasmon assisted microfluidic mixing," *Appl. Phys. Lett.* **92**(12), 124108 (2008) [doi:10.1063/1.2901192].

[3] Y. Hou, J.-S. Kim, S. Ashkenazi, M. O'Donnell, and L. J. Guo, "Optical generation of high frequency ultrasound using two-dimensional gold nanostructure," *Appl. Phys. Lett.* **89**, 093901 (2006) [doi:10.1063/1.2344929].

[4] B. Chance, "Near-infrared images using continuous, phase-modulated, and pulsed light with quantitation of blood and blood oxygenation," *Ann. NY Acad. Sci.* **838**, 29–45 (1998) [doi:10.1111/j.1749-6632.1998.tb08185.x].

[5] M. Suzuki, W. Maekita, K. Kishimoto, S. Teramura, K. Nakajima, K. Kimura, and Y. Taga, "Direct formation of arrays of prolate Ag nanoparticles by dynamic oblique deposition," *Jpn. J. Appl. Phys.* **44**(5), L193–L195 (2005) [doi:10.1143/JJAP.44.L193].

[6] M. Suzuki, W. Maekita, Y. Wada, K. Nakajima, K. Kimura, T. Fukuoka, and Y. Mori, "In-line aligned and bottom-up Ag nanorods for surface-enhanced Raman spectroscopy," *Appl. Phys. Lett.* **88**, 203121 (2006) [doi:10.1063/1.2205149].

[7] A. Leitner, Z. Zhao, H. Brunner, F. Aussenegg, and A. Wokaun, "Optical properties of a metal island film close to a smooth metal-surface," *Appl. Opt.* **32**(1), 102–110 (1993).

[8] H. G. Bingler, H. Brunner, M. Klenke, A. Leitner, F. R. Aussenegg, and A. Wokaun, "Enhanced 2nd-harmonic generation in a silver spacer islands multilayer system," *J. Chem. Phys.* **99**(10), 7499–7505 (1993) [doi:10.1063/1.465730].

[9] D. Steinmullernethl, R. A. Hopfel, A. Leitner, F. R. Aussenegg, and A. Wokaun, "Enhancement of 2nd-harmonic generation in metal islands close to a conducting surface," *Appl. Phys. A* **57**(3), 261–265 (1993).

[10] H. G. Bingler, H. Brunner, A. Leitner, F. R. Aussenegg, and A. Wokaun, "Interference enhanced surface Raman-scattering of adsorbates on a silver-spacer-islands multilayer system," *Mol. Phys.* **85**(3), 587–606 (1995) [doi:10.1080/00268979500101321].

[11] M. Suzuki, K. Nakajima, K. Kimura, T. Fukuoka, and Y. Mori, "Au nanorod arrays tailored for surface-enhanced Raman spectroscopy," *Anal. Sci.* **23**(7), 829 (2007) [doi:10.2116/analsci.23.829].

[12] I. J. Hodgkinson and Q. Wu, *Birefringent Thin Films and Polarizing Elements*, World Scientific, Singapore (1997).

[13] M. Suzuki, W. Maekita, Y. Wada, K. Nagai, K. Nakajima, K. Kimura, T. Fukuoka, and Y. Mori, "Ag nanorod arrays tailored for surface-enhanced Raman imaging in the near-infrared region," *Nanotechnology* **19**(26), 265304 (2008) [doi:10.1088/0957-4484/19/26/265304].

[14] M. Suzuki and Y. Taga, "Numerical study of the effective surface area of obliquely deposited thin films," *J. Appl. Phys.* **90**(11), 5599–5605 (2001) [doi:10.1063/1.1415534].

[15] H. Tamarua, H. Kuwata, H. T. Miyazaki, and K. Miyano, "Resonant light scattering from individual Ag nanoparticles and particle pairs," *Appl. Phys. Lett.* **80**, 1826–1828 (2002) [doi:10.1063/1.1461072].

[16] P. B. Johnson and R. W. Christy, "Optical constants of noble metals," *Phys. Rev. B* **6**(12), 4370 (1972) [doi:10.1103/PhysRevB.6.4370].

[17] I. J. Hodgkinson and Q. Wu, "Serial bideposition of anisotropic thin films with enhanced linear birefringence," *Appl. Opt.* **38**(16), 3621–3625 (1999) [doi:10.1364/AO.38.003621].

[18] Q. H. Wu and I. Hodgkinson, "Transmission-mode perpendicular incidence ellipsometry of anisotropic thin films," *J. Opt.* **25**(2), 43–49 (1994) [doi:10.1088/0150-536X/25/2/001].

[19] M. Suzuki and Y. Taga, "Integrated sculptured thin films," *Jpn. J. Appl. Phys. Part 2* **40**(4A), L358–L359 (2001) [doi:10.1143/JJAP.40.L358].

[20] S.-W. Joo, "Surface-enhanced Raman scattering of 4,4'-bipyridine on gold nanoparticle surfaces," *Vib. Spectrosc.* **34**, 269–273 (2004) [doi:10.1016/j.vibspec.2003.12.006].

Motofumi Suzuki is an associate professor at Kyoto University. He received his bachelor, master and doctor of engineering degrees from Kyoto University in 1986, 1988 and 1998, respectively. His current research interests include the optical properties of nanostructured thin films and the synthesis of novel nanostructures. He is a member of SPIE.